A Combined Order Selection and Parameter Estimation Algorithm for Coupled Harmonics

Gene T. Whipps

U.S. Army Research Laboratory
2800 Powder Mill Road
Adelphi, MD 20783 USA

Randolph L. Moses

Department of Electrical Engineering
The Ohio State University
2015 Neil Avenue
Columbus, OH 43210 USA

Abstract

The problem of estimating the fundamental frequency and the amplitudes and phases of corresponding harmonics is considered. Many battlefield vehicles generate coupled harmonic acoustics. These features are useful in tracking and classifying battlefield targets. As discussed in [1], harmonic line association (HLA) is a feasible approach to target identification in single or multiple target scenarios. In addition, the harmonic line estimates may be useful in improving target tracking and counting. For distributed sensor networks, the harmonic line estimates can also be used in conjunction with direction-of-arrival (DOA) estimates to separate targets temporally and spatially. Once the coupled harmonic parameters are estimated, the residual allows any broadband energy to be exploited.

This work investigates the case with a single source generating frequency coupled harmonics in the presence of Gaussian noise. The parameters of coupled harmonics are estimated using nonlinear least-squares (NLS). Previous works have assumed the number of harmonics is known [2, 3, 4, 5]. In this work, as with [6, 7], the number of harmonics is assumed unknown. The NLS method is combined with order selection methods (such as Rissanen's minimum description length (MDL) [8]), to generate statistically efficient estimates in white and colored noise.

1. Introduction

This document details a combined detection-estimation algorithm for determining the parameters of frequency coupled harmonics. The coupled harmonics are related by a fundamental frequency (FF), denoted ω_0. Estimating the frequencies in harmonic models is a nonlinear process. Usually a frequency is assumed and then linear techniques can be used to estimate the amplitude parameters. However, the accuracy of the estimates depends on the assumed frequency.

Previous work by Dommermuth [6] has shown that the FF can be estimated accurately to within an integer multiple or rational fraction of the true FF. Rational fractions and integer factors of the FF will be referred to as sub-harmonics and super-harmonics, respectively. For estimators based on the minimization of the squared error, the difficulty lies in the multimodal shape of the error (or loss) function. For the coupled harmonic model, the loss function will have deep troughs at multiples of the true FF. The relative levels of the troughs depend on the number of harmonics in the candidate signal and the amplitudes of the harmonics (see, $e.g.$, Figure 2). The mis-estimation of a FF as a sub- or super-harmonic results in large estimate variances. The dependence of the loss function on the FF and the number of harmonics is a motivating factor for this work.

Some previous works, [2, 3, 4, 5], assume the number of harmonics is fixed or known. In [6], combined order selection and FF estimation is also considered. There, estimators are developed assuming a more restrictive model of equal energy harmonics. Consequently, the problem of estimating the amplitudes and phases is not considered. We develop an approach in which we also estimate the amplitudes and phases of a more general coupled harmonic model. We also consider several order selection strategies.

Methods are proposed in [7], similar to those provided here, to jointly estimate the coupled harmonics and autoregressive (AR) noise parameters and model orders. In contrast, we assume the noise power spectral density (PSD) is stationary and known to within a constant level. Assuming the noise model is known may have validity for battlefield acoustics. In some scenarios, long periods of inactivity allows sensors to estimate the local noise properties to a higher degree of accuracy ($i.e.$, large sample lengths) compared to the shorter sample length estimates in [7]. In addition, the algorithms proposed here take advantage of the shape of the loss function in order to reduce the computational complexity.

Algorithms are proposed in [3] and [4] to track the time-varying parameters of coupled harmonics. These algorithms rely on accurate initial FF estimates and assume the number of harmonics is known. In applications where the parameters are slowly varying, the algorithms proposed here can be used to initialize and periodically update the tracking algorithms.

Performance results using simulated data are presented in terms of bias and root-mean-squared error (RMSE). The RMSEs are compared against the large-sample root Cramér-Rao lower bounds (root-CRLBs). Comparisons with the root-CRLBs are made as a function of SNR and number of harmonics. In addition, a qualitative analysis is presented for field data.

The paper is organized as follows. In Section 2, the signal model is presented. In Section 3, the nonlinear parameter estimation procedure is discussed under the assumption the number of harmonics is known. Then, the order selection procedures commonly used to determine the number of narrowband components in a signal are introduced in Section 4. In addition, the proposed combined detection-estimation algorithms for coupled harmonics are presented. Some practical issues related to the algorithms are discussed. Section 5 presents practical numerical examples that demonstrate the statistical properties of the algorithms. In addition, results are compared between parameter estimates and the short-time Fourier transform (STFT) of field measurement data. Finally, concluding remarks and observations are given in Section 6.

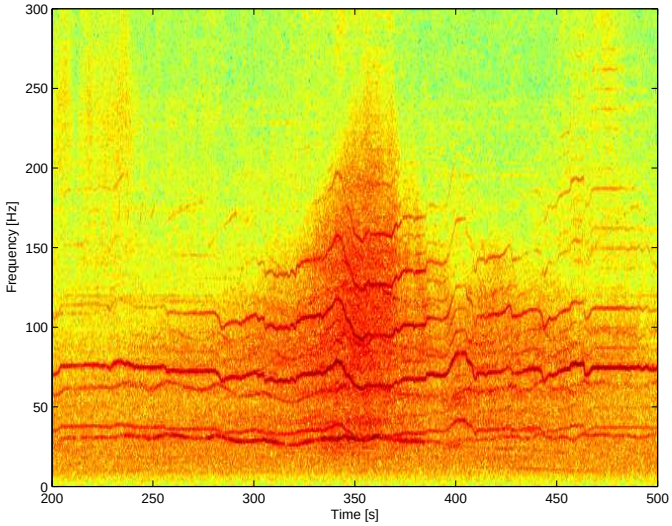

Figure 1: Spectrogram from the acoustic signature of a heavy-tracked vehicle.

2. Signal Model

In this section, the sum-of-harmonics plus broadband noise model is presented. Many physical processes contain periodic and broadband information. Periodicities evident in acoustics are due to, among other things, rotating mechanical components or resonant vibrations. Broadband energy is partly due to the impulsive nature of events or "noise-like" processes, such as turbine engines. Figure 1 is a spectral representation of the measured scalar acoustics of a heavy-tracked vehicle. In addition to the broadband signal, the harmonic structure is evident. Assuming a perfectly calibrated acoustic sensor, the observed signal is

$$\begin{aligned} y(n) &= \sum_{k=1}^{q} \alpha_k \cos\left(k\omega_0 n + \phi_k\right) + \epsilon(n), \\ &= \sum_{k=1}^{q} u_k \cos\left(k\omega_0 n\right) + v_k \sin\left(k\omega_0 n\right) + \epsilon(n), \end{aligned} \tag{1}$$

where $\omega_0 = 2\pi f_0 T$ is the FF satisfying $\omega_0 \in (0, \pi/q)$, q is the number of harmonics present in the signal, $\epsilon(n)$ is modeled as a zero-mean, additive Gaussian noise sequence, n is the sample index, and T is the sampling period. The term $\epsilon(n)$ can also represent noise and un-modeled broadband energy. It is of interest to estimate ω_0, q, the amplitudes $\{\alpha_k\}$, and phases $\{\phi_k\}$. The desired amplitudes and phases are calculated from estimates of the cartesian amplitudes $\{u_k\}$ and $\{v_k\}$ by

$$\begin{aligned} \alpha_k &= \sqrt{u_k^2 + v_k^2}, \\ \phi_k &= \arctan\left(-v_k/u_k\right). \end{aligned} \tag{2}$$

As observed in Figure 1, the FF may be time-varying. Here, it is assumed the FF is constant over an observation window. An observation window of one second is often used for acoustic measurements of vehicles [9].

The observed signal may also be written in matrix form. Let $\mathbf{y}$ be a vector of sampled sensor data for sample indices n = 0,...,$N-1$. Using Equation (1), the harmonic model can be written as

$$\begin{aligned} \mathbf{y} &= \mathbf{C}(\omega_0)\mathbf{u} + \mathbf{S}(\omega_0)\mathbf{v} + \boldsymbol{\epsilon}, \qquad (N \times 1) \\ &= \mathbf{A}(\omega_0)\boldsymbol{\beta} + \boldsymbol{\epsilon}, \end{aligned} \tag{3}$$

where

$$\begin{aligned} \mathbf{u} &= [u_1, \ldots, u_q]^T, \qquad (q \times 1) \\ \mathbf{v} &= [v_1, \ldots, v_q]^T, \qquad (q \times 1) \end{aligned} \tag{4}$$

are the amplitude vectors, and the elements of the $(N \times q)$ matrices $\mathbf{C}(\omega)$ and $\mathbf{S}(\omega)$ are given by

$$\begin{aligned} [\mathbf{C}(\omega)]_{n,k} &= \cos(k\omega n + \varphi_k), \qquad 0 \le n \le N-1 \\ [\mathbf{S}(\omega)]_{n,k} &= \sin(k\omega n + \varphi_k), \qquad 1 \le k \le q \end{aligned} \tag{5}$$

where n and k are the row and column indices, respectively, and $\varphi_k = k\omega(N-1)/2$. The phase term, φ_k, defines the phase at the middle of the observation window and guarantees $\mathbf{C}(\omega)^T\mathbf{S}(\omega) = \mathbf{0}$. From the second line in Equation (3), it follows that $\mathbf{A}(\omega) = [\mathbf{C}(\omega), \mathbf{S}(\omega)]$ and $\boldsymbol{\beta} = [\mathbf{u}^T, \mathbf{v}^T]^T$. Amplitude and phase vectors are defined as

$$\begin{aligned} \boldsymbol{\alpha} &= [\alpha_1, \ldots, \alpha_q]^T, \qquad (q \times 1) \\ \boldsymbol{\phi} &= [\phi_1, \ldots, \phi_q]^T. \qquad (q \times 1) \end{aligned} \tag{6}$$

The cartesian amplitude vectors $\mathbf{u}$ and $\mathbf{v}$ are viewed as the rectangular coordinates in the signal subspace $\langle \mathbf{A}(\omega_0) \rangle$ spanned by the columns of $\mathbf{A}(\omega_0)$. The rectangular coordinates are related to their polar counterparts by

$$\begin{aligned} \mathbf{u} &= \boldsymbol{\alpha} \cdot \cos(\boldsymbol{\phi}), \qquad (q \times 1) \\ \mathbf{v} &= -\boldsymbol{\alpha} \cdot \sin(\boldsymbol{\phi}), \qquad (q \times 1) \end{aligned} \tag{7}$$

where $\mathbf{x} \cdot \mathbf{z}$ is the scalar product of $(m \times 1)$ vectors $\mathbf{x}$ and $\mathbf{z}$, and $\cos(\mathbf{x}) = [\cos(x_1), \ldots, \cos(x_m)]^T$ with $\sin(\mathbf{x})$ similarly defined.

The last term on the right hand side of Equation (3) is a vector of noise samples distributed as $\boldsymbol{\epsilon} \sim \mathcal{N}(\mathbf{0}, \boldsymbol{\Sigma})$. The harmonic signal and broadband noise are considered statistically independent. The noise is modeled as a stationary autoregression. Formally, the AR noise is described as

$$\epsilon(n) = \frac{1}{A(z)} e(n), \tag{8}$$

where $A(z)$ is a stable, rational linear filter and $e(n)$ is zero-mean white noise with variance σ_{AR}^2. The filter $A(z)$ has the form

$$A(z) = 1 + a_1 z^{-1} + \ldots + a_p z^{-p}, \tag{9}$$

where z^{-1} is the unit delay operator ($e.g.$, $z^{-p}x(n) = x(n-p)$). The parameters of $A(z)$ are then given as

$$\boldsymbol{\theta}_{AR} = [a_1, \ldots, a_p]^T. \qquad (p \times 1) \tag{10}$$

If the AR parameters are not known, then they must be estimated. AR parameter estimation techniques are treated in [10]. In some applications, the degree of accuracy of the AR parameter estimates is greater than that of the signal parameter estimates ($i.e.$, $M \gg N$, where M is the data length used in estimating $\boldsymbol{\theta}_{AR}$). In this work, it is assumed $\boldsymbol{\theta}_{AR}$ is known and the data is whitened prior to estimation. Given $\boldsymbol{\theta}_{AR}$, the whitened samples are generated by filtering the observations with $A(z)$ ($i.e.$, $\tilde{y}(n) = A(z)y(n)$). After this pre-whitening procedure, the harmonic model is given by

$$\tilde{\mathbf{y}} = \mathbf{C}(\omega_0)\tilde{\mathbf{u}} + \mathbf{S}(\omega_0)\tilde{\mathbf{v}} + \tilde{\boldsymbol{\epsilon}}, \qquad (N \times 1) \tag{11}$$

where $\tilde{\boldsymbol{\epsilon}} \sim \mathcal{N}(\mathbf{0}, \tilde{\sigma}^2\mathbf{I})$. After computing the estimates of $\tilde{\mathbf{u}}$ and $\tilde{\mathbf{v}}$, the estimates of $\boldsymbol{\alpha}$ and $\boldsymbol{\phi}$ are determined by using Equation (2) and then removing the effects of the whitening filter. It follows that the estimation techniques for both cases, white or AR noise, share a common structure. Consequently, without loss of generality, it is assumed $\boldsymbol{\Sigma} = \sigma^2\mathbf{I}$ in the following derivations.

3. Coupled Harmonic Parameter Estimation

It is desired to estimate the parameter vector

$$\boldsymbol{\theta}^{pol} = [\omega_0, \alpha_1, \ldots, \alpha_q, \phi_1, \ldots, \phi_q]^T. \qquad (2q + 1 \times 1) \tag{12}$$

However, the signal is a nonlinear function of the phase parameters, $\boldsymbol{\phi}$. Consequently, the estimators are given in terms of the cartesian amplitudes. Defining the vector

$$\boldsymbol{\theta}^{rect} = [\omega_0, u_1, \ldots, u_q, v_1, \ldots, v_q]^T, \qquad (2q + 1 \times 1) \tag{13}$$

the maximum likelihood estimate (MLE) of $\boldsymbol{\theta} = \boldsymbol{\theta}^{rect}$ is found by minimizing the negative log-likelihood function given by

$$J(\boldsymbol{\theta}) = \frac{N}{2}\ln(2\pi) + \frac{1}{2}\ln(\det\boldsymbol{\Sigma}) + \frac{1}{2}(\mathbf{y} - \mathbf{s}(\boldsymbol{\theta}))^T\boldsymbol{\Sigma}^{-1}(\mathbf{y} - \mathbf{s}(\boldsymbol{\theta})), \tag{14}$$

where $\mathbf{s}(\boldsymbol{\theta}) = \mathbf{A}(\boldsymbol{\omega})\boldsymbol{\beta}$.

The number of parameters to be estimated in general sinusoidal summation models with q components ($i.e.$, $\{\omega_k, v_k, u_k\}_{k=1}^q$) is $3q$. However, in the coupled harmonics model, the number of parameters is reduced to $2q+1$ as all frequency components are described by a single parameter, ω_0. The following section describes the procedure used to estimate $\boldsymbol{\theta}$ from N finite samples.

3.1 Maximum Likelihood Estimation

With the assumption of white noise ($\boldsymbol{\Sigma} = \sigma^2\mathbf{I}$), the parameter vector $\boldsymbol{\theta}$ that minimizes $J(\boldsymbol{\theta})$ also minimizes

$$\begin{aligned} L(\boldsymbol{\theta}) &= \|\mathbf{y} - \mathbf{s}(\boldsymbol{\theta})\|^2, \\ &= \|\boldsymbol{\epsilon}\|^2. \end{aligned} \tag{15}$$

Equation (15) is the squared norm of the difference between the measurement and the signal model. Note that the constant term due to the noise variance is ignored since it does not impact the minimization of $J(\boldsymbol{\theta})$. For the chosen model of $s(n)$, the estimation of the parameter vector $\boldsymbol{\theta}$ is a highly nonlinear process. However, the minimization of Equation (15) can be achieved by the method of least-squares (LS) if ω_0 and q are assumed known. In practice, a grid search over candidate ω is performed. For a candidate ω and a fixed q, the cartesian amplitude estimates are found by

$$\{\hat{\mathbf{u}}(\omega), \hat{\mathbf{v}}(\omega)\} = \arg \min_{\{\mathbf{u},\mathbf{v}\}} \|\mathbf{y} - \mathbf{C}(\omega)\mathbf{u} - \mathbf{S}(\omega)\mathbf{v}\|^2 . \tag{16}$$

The LS solutions to Equation (16) can be decoupled and obtained by

$$\begin{aligned} \hat{\mathbf{u}} &= \left(\mathbf{C}^T\mathbf{C}\right)^{-1}\mathbf{C}^T\mathbf{y}, \\ \hat{\mathbf{v}} &= \left(\mathbf{S}^T\mathbf{S}\right)^{-1}\mathbf{S}^T\mathbf{y}, \end{aligned} \tag{17}$$

where the dependance on the frequency has been suppressed to simplify the notation. Given $\hat{\mathbf{u}}$ and $\hat{\mathbf{v}}$, the amplitude estimates $\{\hat{\alpha}_k\}$ and phase estimates $\{\hat{\phi}_k\}$ are found using Equation (2).

It is straightforward to show that the product $\mathbf{A}^T\mathbf{A}$ must be block diagonal to ensure exact decoupling of the amplitude estimates. Diagonality is guaranteed by defining the phase of the candidate signal at the center of the observation window. Otherwise, the above product is approximately block diagonal for large data lengths. As noted in [2], there is a computational benefit from decoupling the amplitude estimates. Assuming $N \gg q$, the complexity of computing the LS estimates in Equation (17) is $\mathcal{O}(2Nq^2)$. The complexity more than doubles without decoupling.

Using the LS amplitude estimates of Equation (17), the loss function for fundamental frequency estimates (FFEs) is given by

$$\begin{aligned} L(\omega) &= \|\mathbf{y} - \mathbf{C}\hat{\mathbf{u}} - \mathbf{S}\hat{\mathbf{v}}\|^2 , \\ &= \left\|\mathbf{y} - \mathbf{C}(\mathbf{C}^T\mathbf{C})^{-1}\mathbf{C}^T\mathbf{y} - \mathbf{S}(\mathbf{S}^T\mathbf{S})^{-1}\mathbf{S}^T\mathbf{y}\right\|^2 , \\ &= \left\|\mathbf{y} - \mathbf{A}(\mathbf{A}\mathbf{A})^{-1}\mathbf{A}^T\mathbf{y}\right\|^2 , \\ &= \mathbf{y}^T\mathbf{P}^{\perp}\mathbf{y}, \end{aligned} \tag{18}$$

where $\mathbf{P}^{\perp} = \mathbf{I} - \mathbf{A}(\mathbf{A}^T\mathbf{A})^{-1}\mathbf{A}^T = \mathbf{I} - \mathbf{P}$ projects the observation into the null space of $\mathbf{A}$. Finally, the maximum likelihood (ML) FFE is given by

$$\begin{aligned} \hat{\omega}_0 &= \arg\min_{\omega} L(\omega), \\ &= \arg\min_{\omega} \mathbf{y}^T\mathbf{P}^{\perp}\mathbf{y}. \end{aligned} \tag{19}$$

This minimization procedure is also known as the nonlinear least-squares (NLS) method. In determining $\hat{\omega}_0$, the estimator attempts to minimize (maximize) the energy in the null space (column space) of $\mathbf{A}$. Although there are $2q + 1$ free parameters, the NLS method reduces the parameter search to a 1-dimensional (1-D) search. Once $\hat{\omega}_0$ has been computed, the ML cartesian amplitude estimates are simply given by Equation (17).

Now, an approximation to the NLS method is considered. For large sample lengths ($i.e.$, $N \to \infty$) the approximations $\mathbf{C}^T\mathbf{C} \approx \frac{N}{2}\mathbf{I}_q$ and $\mathbf{S}^T\mathbf{S} \approx \frac{N}{2}\mathbf{I}_q$, where $\mathbf{I}_m$ is the $(m \times m)$ identity matrix, are made.

Therefore, the loss function of Equation (18) can be approximated by

$$\begin{aligned} L(\omega) &\approx \left\| \mathbf{y} - \frac{2}{N}\mathbf{C}\mathbf{C}^T\mathbf{y} - \frac{2}{N}\mathbf{S}\mathbf{S}^T\mathbf{y} \right\|^2, \\ &= \left\| \left(\mathbf{I} - \frac{2}{N}\mathbf{A}\mathbf{A}^T \right) \mathbf{y} \right\|^2. \end{aligned} \tag{20}$$

The FFEs from the minimization of Equation (20) for finite data lengths are not ML, but are however asymptotically efficient in data length. Furthermore, the approximation to the ML FFE provides computational savings when $q > 2$. The complexity of Equation (18) is $\mathcal{O}(2Nq^2)$, whereas the complexity of Equation (20) is $\mathcal{O}(4Nq)$.

As demonstrated by [11] for complex sinusoids and [12] for real sinusoids, the NLS method still gives consistent, although no longer ML, parameter estimates in colored Gaussian noise without the pre-whitening step. However, the order selection methods used here, as discussed below, require the noise be uncorrelated. Therefore, pre-whitening is a necessary step in the proposed algorithm.

3.2 Cramér-Rao Bounds

The Cramér-Rao lower bound (CRLB) provides a good comparison tool for evaluating estimator performance. The CRLBs, which bound the minimum achievable variance of unbiased estimators, have been well developed for harmonic retrieval problems in white [2, 13, 14], and correlated [2, 11, 15] Gaussian noise. The CRLBs for frequency coupled harmonics are developed in [2] and [14]. The CRLBs of coupled harmonics are also given here. The finite- and large-sample (as $N \to \infty$) CRLBs are developed in Appendix A of [16]. The large-sample Cramér-Rao lower bounds for unbiased estimators of the amplitudes, phases, and FF are [2]

$$\sigma^2_\infty(\hat{\alpha}_k) = \frac{2\sigma_k^2}{N}, \tag{21}$$

$$\sigma^2_\infty(\hat{\phi}_k) = \frac{2\sigma_k^2}{N\alpha_k^2}, \tag{22}$$

$$\sigma^2_\infty(\hat{\omega}_0) = \frac{12}{N^3}\left(\sum_{k=1}^{q} \frac{k^2\alpha_k^2}{2\sigma_k^2} \right)^{-1}. \tag{23}$$

In the case of white noise, $\sigma_k^2 = \sigma^2$. For colored noise, the local variance is given by $\sigma_k^2 = |H(e^{jk\omega_0})|^2\sigma^2$, where $H(e^{j\omega}) = |A(e^{j\omega})|^{-1}\angle A(e^{-j\omega})$.

The finite-sample CRLB for an individual parameter is denoted by $\sigma^2_N(\cdot)$. The reason for using σ^2_∞ in this work is twofold: σ^2_∞ is easier to compute than σ^2_N, and σ^2_∞ approximates σ^2_N well when the minimum frequency separation is sufficiently large [13]. The minimum frequency separation for multi-harmonic models is $\omega_{min} > 2\pi/N$ [13]. For the coupled harmonic model, the critical value bounds the minimum resolvable FF.

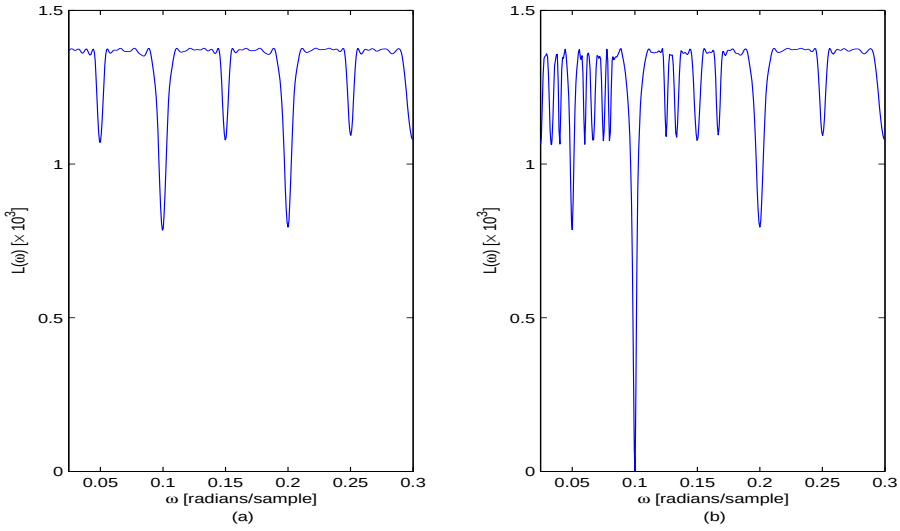

Figure 2: Loss function for a noiseless signal and the system order set to (a) $r = 2$ (under-set order) and (b) $r = 5$ (correct order) in estimating the FF. The actual number of harmonics is $q = 5$ with $\omega_0 = 0.1$ radians/sample and uniform harmonic signal amplitudes.

3.3 Loss Function Characteristics

The frequency estimate defined in Equation (19) is derived under the assumption q is known. If the true number of harmonic lines is not known, FFEs can be highly biased if the number of columns, r, in Equation (5) is set incorrectly ($i.e.$, $r \neq q$). Here, r is referred to as the system order. The loss function defined by Equation (18) is multi-modal. This property of the loss function gives rise to biased frequency estimates when the system order is incorrect. Two examples that follow demonstrate this behavior.

Figure 2 shows two plots for the loss function of the frequency estimates of a noiseless signal. The true FF is $\omega_0 = 0.1$ radians/sample and the true number of harmonics is $q = 5$. Also, the amplitudes of the harmonics are set to unity and the phases are random. The simulated signals are generated from a 1 second window with $N = 512$ samples. The loss function values for candidate frequencies at 0.1 and 0.2 radians/sample are nearly equal when the system order is set to $r = 2$, as shown in Figure 2(a). In the presence of noise, the global minimum of the loss function may well be $2\omega_0$ for this case. As a result, Equation (18) could give highly biased FFEs. If the number of harmonics in the signal is known, then Figure 2(b) is representative of the expected loss function for candidate frequencies. Here, the global minimum corresponds to the correct FF. A similar situation occurs for other amplitude models [16]. As demonstrated in [16], the global minimum may correspond to $\omega_0/2$ for an over-set system order.

The frequency estimates using Equation (18), when biased, are multiples of the true FF for sufficiently high SNR and frequency resolution. Conditions for the frequency resolution are discussed below. For the coupled harmonic model, the initial estimates are given by the NLS solution for a reasonable choice of r. Then, an accurate estimate of the true FF can be determined by the use of order estimates.

As determined by [13], harmonics embedded in noise can be estimated very accurately given good initial estimates. This is evident in the deep, narrow troughs in Figure 2. This also suggests that a rather fine search

grid is required to ensure a candidate frequency lands in a trough of the loss function. So, it is of interest to determine an adequate frequency resolution. In what follows is a rudimentary guide to determine a suitable frequency search grid spacing.

To simplify the analysis, it is assumed the coupled harmonics have unit amplitudes and q is known. Due to sampling with a finite length window, each harmonic has an associated spectrum. For a rectangular window, each harmonic will have a $\sin(\omega N/2)/\sin(\omega/2)$ spectrum centered at the harmonic frequency. Consequently, each spectrum has a corresponding main beam in which most of the energy is located. The width of the main beam is defined here using the beamwidth between the first nulls (BWBN). The BWBN for the spectrum of a rectangular window is $4\pi/N$.

When the candidate FF is offset from the actual FF by $\delta\omega$, the spectrum of the k^{th} candidate harmonic is shifted in frequency by $k\delta\omega$ from that of the k^{th} true harmonic. When $k\delta\omega = 2\pi/N$, the k^{th} candidate spectrum is orthogonal to the spectrums of the true harmonic frequencies ($\mathbf{C}(\omega_0)^T\mathbf{C}(\omega_0 + 2\pi/kN)_k = \mathbf{0}$ and $\mathbf{S}(\omega_0)^T\mathbf{S}(\omega_0 + 2\pi/kN)_k = \mathbf{0}$, where $\mathbf{C}(\omega)_k$ and $\mathbf{S}(\omega)_k$ are the k^{th} columns of $\mathbf{C}(\omega)$ and $\mathbf{S}(\omega)$, respectively). Consequently, no energy from the k^{th} candidate harmonic contributes in minimizing the NLS loss function. In addition, orthogonality for the k^{th} harmonic also holds when $\delta\omega$ is an integer multiple of $2\pi/kN$. So for example, when q is even and $\delta\omega = 4\pi/qN$, the spectrums of the middle and last candidate harmonics are orthogonal to each of those in the true signal. Incidentally, when $\delta\omega = 4\pi/qN$, the spectral main lobes from the last candidate and true harmonic no longer overlap. It follows that the loss function evaluated at candidate frequencies in the vicinity of the true fundamental with increasing offset in the range $2\pi/qN < \delta\omega < 4\pi/qN$ will take on increasingly large values. As a result, the suggested frequency search grid spacing is $\Delta\omega = BWBN/2q$.

3.4 Comments

Dommermuth [6] proposed a loss function that averages the squared errors over possibly non-overlapping time windows. However, time averaging may increase estimate variances because of the large sample requirements for the NLS method and the increased potential for model mismatches. A similar but alternate method could be used in sensor array applications. Instead of averaging $L(\omega)$ over data blocks, the loss function can be averaged over sensors. It should be noted that this alternative averaging approach assumes parameter estimation is done prior to beamforming.

4. Model Order Selection

In general, the number of significant harmonics is unknown. Therefore, it is of interest to use the model order information to properly choose the correct FF. Several standard order selection techniques are well suited to this task. These methods include Akaike's information criterion (AIC), Rissanen's minimum description length (MDL), and maximum $a\ posteriori$ probability (MAP) [17]. AIC and MDL are derived from Information Theoretic Criterion (ITC), whereas MAP is derived from asymptotic Bayesian decision theory. Each method has a similar form with a data term and a penalty term. The penalty term accounts for the reduced fit error when the model order is overestimated. For sinusoidal summation models, the order

selection criteria have the form [18]

$$\hat{q}_{AIC} = \arg\min_r \left\{ N \ln J(\hat{\boldsymbol{\theta}}) + 3r \right\}, \tag{24}$$

$$\hat{q}_{MDL} = \arg\min_r \left\{ N \ln J(\hat{\boldsymbol{\theta}}) + \frac{3r}{2} \ln N \right\}, \tag{25}$$

$$\hat{q}_{MAP} = \arg\min_r \left\{ N \ln J(\hat{\boldsymbol{\theta}}) + \frac{5r}{2} \ln N \right\}, \tag{26}$$

where $J(\boldsymbol{\theta})$ is the negative log-likelihood function evaluated at the ML parameter vector $\hat{\boldsymbol{\theta}}$ and $\hat{q}$ is the estimate of the number of sinusoids. Each respective method is denoted by the corresponding subscript. The number of free parameters in this case is $3q$. However, the coupled harmonic model has $2q + 1$ free parameters. The MAP criterion penalizes each unknown amplitude and phase parameter by $\frac{1}{2} \ln N$ and each unknown frequency by $\frac{3}{2} \ln N$ [17]. As a result, the order selection criteria for the coupled harmonic model are

$$\hat{q}_{AIC} = \arg\min_r \left\{ N \ln J(\hat{\boldsymbol{\theta}}) + 2r + 1 \right\} = \arg\min_r \left\{ N \ln J(\hat{\boldsymbol{\theta}}) + 2r \right\}, \tag{27}$$

$$\hat{q}_{MDL} = \arg\min_r \left\{ N \ln J(\hat{\boldsymbol{\theta}}) + \frac{2r+1}{2} \ln N \right\} = \arg\min_r \left\{ N \ln J(\hat{\boldsymbol{\theta}}) + r \ln N \right\}, \tag{28}$$

$$\hat{q}_{MAP} = \arg\min_r \left\{ N \ln J(\hat{\boldsymbol{\theta}}) + \frac{2r+3}{2} \ln N \right\} = \arg\min_r \left\{ N \ln J(\hat{\boldsymbol{\theta}}) + r \ln N \right\}, \tag{29}$$

where $J(\boldsymbol{\theta})$ is defined by Equation (14). The second equality in the three equations above are obtained by removing terms that do not depend on r. Note that the MDL and MAP criteria are equivalent. They they differ from AIC by a factor of $\frac{1}{2} \ln N$ in the second term. The second term penalizes large model orders, so in general AIC tends to give higher model orders than MDL.

The above decision rules were developed under a white Gaussian noise assumption. Another selection rule, proposed by Wang in [19], for the colored noise case has the form

$$\hat{q}_{COL} = \arg\min_r \left\{ N \ln J(\hat{\boldsymbol{\theta}}) + \frac{cr}{2} \ln N \right\}, \tag{30}$$

where c is a constant greater than a threshold γ, which depends on the characteristics of the noise.

It was noted in [17] that Equation (30) can give inconsistent estimates based on the choice of c. In addition, it was determined in [20] that AIC produces inconsistent estimates and tends to overestimate the model order, whereas MDL yields consistent estimates for large sample records. Due to the consistency of MDL, it is the preferred order selection method considered here. The rule proposed by Wang is not examined further, but is a possible extension of this work.

The combined detection-estimation algorithm for coupled harmonics has the form

$$\begin{aligned} \{\hat{\boldsymbol{\theta}}, \hat{q}\} &= \arg\min_{\{\boldsymbol{\theta}, r\}} \{ N \ln J(\boldsymbol{\theta}) + r \ln N \}, \\ &= \arg\min_{\{\boldsymbol{\theta}, r\}} \{ N \ln L(\boldsymbol{\theta}) + r \ln N \}, \end{aligned} \tag{31}$$

where the MDL criteria represents the detection component and $L(\boldsymbol{\theta})$, given by Equation (15), represents the estimation component. Since the estimation component can be reduced to a 1-D search it follows that

the combined algorithm can be reduced to a 2-D search. Thus, combining Equation (18) with Equation (31) the FF and order estimates are found by

$$\begin{aligned}\{\hat{\omega}_0, \hat{q}\} &= \arg\min_{\{\omega,r\}} N\ln(\mathbf{y}^T\mathbf{P}^{\perp}\mathbf{y}) + r\ln N, \\ &= \arg\min_{\{\omega,r\}} h(\omega, r). \end{aligned} \tag{32}$$

Then, the amplitude estimates are generated using Equation (17) with the estimates $\hat{\omega}_0$ and $\hat{q}$. When $\hat{q} = q$, $\hat{\omega}_0$ is the MLE. Otherwise, when $\hat{q} \neq q$, Equation (32) can still be used to generate statistically efficient FFEs ($i.e.$, var($\hat{\omega}_0$) $= \sigma^2_{\infty}(\omega_0)$), as it will be shown through simulations. In the case of colored noise, $\mathbf{y}$ is simply replaced by $\tilde{\mathbf{y}}$ in Equation (32).

4.1 Proposed Algorithm

It is important to estimate both the parameter set and model order together. Since the order selection methods depend on the parameter estimates, the order estimates may be highly biased when the FF estimates are biased. This frequency-order dependence is evident in Figure 3. The simulated signal is composed of $q = 7$ harmonics with $\omega_0 = 0.1$ radians/sample. The SNR, defined as $\rho = \boldsymbol{\alpha}^T\boldsymbol{\alpha}/2\sigma^2$, of the simulated white noise is set to $\rho = 3$dB. Each curve in Figure 3 represents the loss function defined by Equation (32) evaluated at a fixed frequency (precisely $\omega_0/3$, $\omega_0/2$, ω_0, $2\omega_0$, $3\omega_0$) for a range of $r \in [2, \min(32, r_{nyq})]$, where $r_{nyq} < \lfloor \pi/\omega \rfloor$ satisfies the Nyquist criterion. As seen in Figure 3, the global minimum corresponds to the correct FF and order. Notice that the minimum of the loss function for a frequency other than the correct FF does not correspond to the correct order. Also apparent in Figure 3 is that the loss function evaluated at ω_0 has a range of r such that, although not the global minimum, the function is less than the minimum at candidate frequencies at the same order.

In practice, the procedure of Equation (32) requires a fine grid search over frequency and all possible integer orders. This approach is computationally burdensome. However, it is possible to find the global minimum with a reduced search grid. Recall the general pattern of the loss function versus frequency (no order selection). As seen in Figure 2, deep, narrow troughs occur at the FF, sub- and super-harmonics. As noted previously, this suggests that these frequencies, although not necessarily the true FF, can be estimated with a high degree of accuracy. With r properly set, an initial FF estimate, denoted $\hat{\omega}_i$, will likely correspond to the true FF or multiple thereof. A reduced frequency search set can be defined using the initial frequency estimate ($e.g.$, $\omega \in \{\hat{\omega}_i/2, \hat{\omega}_i, 2\hat{\omega}_i, 3\hat{\omega}_i\}$). Then, the loss function can be minimized over the new frequency set and model order. This initialization and the combined order selection/estimation is the basis behind the algorithms proposed in this paper. The first algorithm is detailed in Table 1. The algorithm is referred to as the NLS-MDL method. The algorithm is basically a two stage procedure: first, generate an initial FFE, and, second, generate the order and parameter vector estimates.

It is assumed that the signals are anti-alias filtered and any DC bias is removed. Therefore, the harmonics must satisfy $k\omega_0 \in (0, \pi)$ for $k \in \{1, \ldots, q\}$. This requirement bounds above the model order corresponding to each FF. However, high orders are possible for lower fundamental frequencies. Therefore, order searches for lower frequencies require more computations than for higher frequencies. In general, the frequency and order search regions would normally be confined by prior knowledge. For example, the frequency search region for the simulations in this work is uniformly confined to $f \in \Lambda_f = [2, 25]$ Hz, which is a relaxed region based on prior knowledge on battlefield acoustics [1]. It has also been determined that a sampling rate on the order of 0.5-1 kHz is sufficient [1, 9] for most acoustic vehicle detection and classification

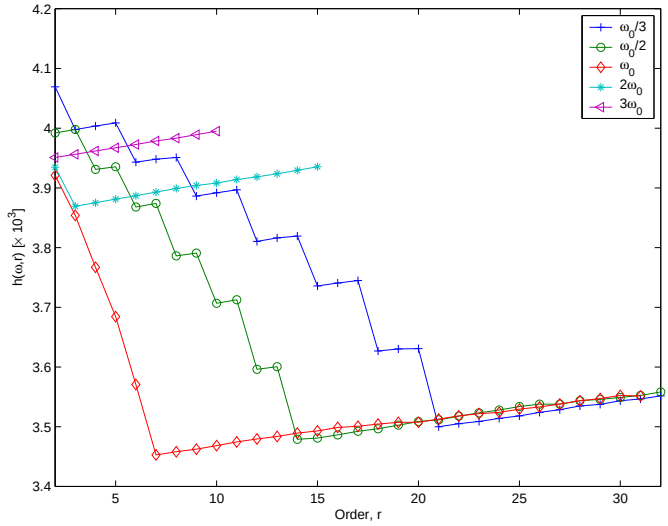

Figure 3: Loss function for a noisy signal using MDL, evaluated at exact values of $\omega_0/3$, $\omega_0/2$, ω_0, $2\omega_0$, and $3\omega_0$, with $\omega_0 = 0.1$ radians/sample. The true number of harmonics is $q = 7$ with uniform amplitudes and $\rho = 3$ dB.

applications. On the other hand, order estimates presented here are upper bounded by the criterion $r_{ub} = \min(r_{max}, r_{nyq})$, where r_{max} is chosen to minimize computations and as a practical limit. Alternatively, to employ less $ad\ hoc$ means, methods such as those proposed by [18] could be implemented to bound the order search region.

The initial estimates in Steps 2 and 3 are generated using likely over-set system orders. Assuming r_{max} is set properly, over-setting the system order ensures that initial FFEs have minimal variance and the mean corresponds to the true FF or a sub-harmonic. Then, any large FFE bias is removed using order selection, hence the procedure in Step 5.

Table 1: Summary of the NLS-MDL Algorithm.

1. Pre-whiten the samples if the noise is correlated using the known AR model by $\tilde{y}(n) = A(z)y(n)$.
2. Obtain an initial estimate, $\tilde{\omega}_i$, of the FF using Equation (18) with a fine frequency search grid from Λ_ω and r set to r_{ub}.
3. Compute a refined initial estimate, $\hat{\omega}_i$, using an optimization technique ($e.g.$, $fminbnd$ in MATLAB), Equation (18), and r set to r_{ub}.
4. Create a new frequency search set from the refined estimate:
   $\Lambda_{\omega_i} = \{\omega = \alpha\hat{\omega}_i | \alpha \in \{1/b\} \cup \{b\}, b \in \mathbb{Z}\} \subset \Lambda_\omega$.
5. Minimize Equation (32) over Λ_{ω_i} and candidate orders in $\Lambda_r = \{2, 3, \ldots, r_{ub}\}$ to get $\hat{\omega}_0$ and $\hat{q}$.
6. Finally, use Equations (17) and (2) with $\hat{\omega}_0$ and $\hat{q}$ to get estimates $\hat{\boldsymbol{\alpha}}$ and $\hat{\boldsymbol{\phi}}$.
7. Remove the effects of pre-whitening from $\hat{\boldsymbol{\alpha}}$ and $\hat{\boldsymbol{\phi}}$. If the noise is white, skip Steps 1 and 7.

A second algorithm, referred to as ANLS-MDL, utilizes the approximated NLS method of Equation (20). The ANLS-MDL algorithm substitutes Equation (20) for (18) in Step 3 of the NLS-MDL algorithm. Also, Equation (20) is combined with Equation (31), which is then substituted for Equation (32) in Step 5. It was determined empirically that the estimate variance of ANLS-MDL is improved by repeating Step 3 with Equation (20) and $r = \hat{q}$ after Step 5. Repeating Step 3 after Step 5 for NLS-MDL does not provide any noticeable improvement.

5. Numerical Results

5.1 Synthetic Data Results

The following are numerical examples that demonstrate statistical properties of the combined detection-estimation algorithm. This study compares the NLS-MDL algorithm with ANLS-MDL and NLS with known or fixed order. The algorithms are examined with simulated correlated Gaussian noise. Results for simulations with white noise are presented in [16].

First, the performance of each algorithm is tested against the large-sample Cramér-Rao lower bounds of Equations (21)-(23) on estimate variances versus SNR. Then, the algorithms are compared against the CRLBs as the true number of harmonics vary. Comparisons are made between the estimate RMSEs and the corresponding large-sample root-CRLBs ($i.e.$, $\sqrt{\sigma^2_\infty(\hat{\omega}_0)}$). The root-CRLBs will simply be referred to as the CRLBs.

The simulation parameters common to the simulations are as follows:

- The sampling period T is set to 1/512 s.
- The FF is $\omega_0 = 0.1$ radians/sample.
- One amplitude model is examined: $1/\sqrt{\omega}$. A uniform amplitude model is also considered in [16].
- The phases are set to $\phi_k = k\pi/100$.
- The maximum order in the search range is set to $r_{ub} = \min(32, \lfloor \pi/\omega \rfloor)$.
- The frequency search range is set to $\omega \in \Lambda_\omega = [\pi/128, 25\pi/256]$ radians/sample ([2,25] Hz) with a frequency resolution of $\pi/8N$ radians/sample ($1/8$ Hz).
- The simulation results are generated from 500 Monte-Carlo simulations.

5.1.1 Algorithm Performance versus SNR in Colored Noise

In this section, NLS-MDL and ANLS-MDL are compared with NLS with the correct order ($i.e.$, $r = q$). The NLS method with $r = q$ will simply be referred to as NLS. The CRLBs in this case are calculated using Equations (21)-(23) with the local noise variance defined as $\sigma_k^2 = |H(e^{jk\omega_0})|^2\sigma^2$. The following results are generated using pre-whitening in Step 1 of the NLS-MDL and ANLS-MDL algorithms.

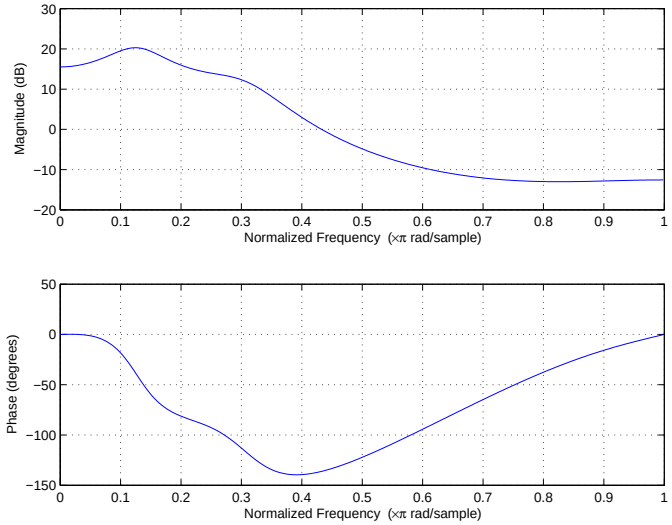

Figure 4: Magnitude (top) and phase (bottom) response of the coloring filter, $H(e^{j\omega})$.

The noise is generated by filtering zero-mean, unit variance Gaussian noise with a fifth order AR coloring filter given by

$$H(z) \approx \frac{1}{1 - 2.0z^{-1} + 1.57z^{-2} - 0.28z^{-3} - 0.36z^{-4} + 0.23z^{-5}}, \tag{33}$$

and then scaled by $\sigma = (\boldsymbol{\alpha}^T\boldsymbol{\alpha}/2\rho\sigma_{AR}^2)^{1/2}$ to achieve the desired SNR. The choice of this model is based on measurements collected at Aberdeen Proving Grounds (APG). The lowpass filter represented by Equation (33) is specific to the local environment at the time in which the measurements were recorded. However, a model needed to be adopted for these simulations. An extension of this work may include a performance analysis with the use of bandpass and/or highpass coloring filters. The frequency response of the coloring filter of Equation (33) is plotted in Figure 4.

For the $1/\sqrt{\omega}$ amplitude model, the absolute value of bias and the RMSE of the frequency estimates are plotted in Figures 5(a) and (b). The RMSEs of the amplitudes and phases for the first harmonic are plotted in Figures 5(c) and (d), respectively. In each figure of estimate RMSE the results are shown with the corresponding root-CRLB.

As seen from Figure 5, the RMSEs from each algorithm correspond well with the CRLB for a large range of SNRs. The estimation accuracy of the NLS-MDL and ANLS-MDL algorithms degrades rapidly below 4 dB SNR. The performance of the NLS algorithm does not diverge from the CRLB for decreasing SNR until approximately 0 dB. Note that number of harmonics of NLS is set to the correct number. It follows that the loss in performance of the NLS-MDL and ANLS-MDL between 0 and 4 dB SNR is mainly due to the uncertainty in the unknown number of harmonics.

The 4 dB SNR threshold for the NLS-MDL and ANLS-MDL methods is the same for a uniform amplitude model and is slightly higher than the threshold in the white noise case [16]. On the other hand, fewer than 1% of the FFEs from NLS-MDL and ANLS-MDL constitute outlying estimates at 0 dB SNR. As shown in [16], the outlying FFEs correspond to outlying order estimates.

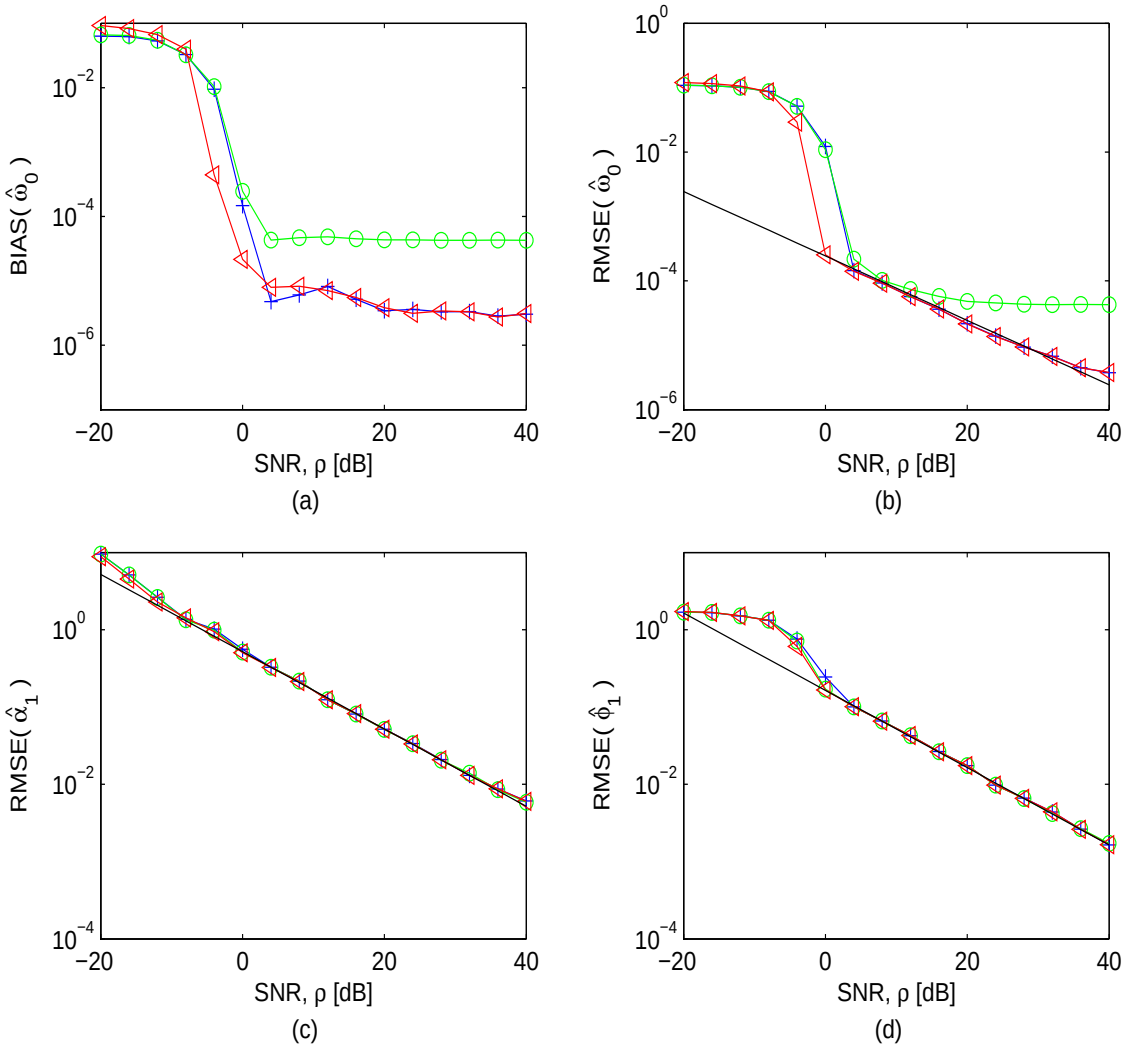

Figure 5: Parameter estimate results for the $1/\sqrt{\omega}$ amplitude model versus SNR in correlated noise: FFE (a) bias and (b) RMSE, along with (c) amplitude and (d) phase estimate RMSEs for the 1^{st} harmonic. The estimates are generated using (+) NLS-MDL, ($\circ$) ANLS-MDL, and ($\triangleleft$) NLS with $r = q$. The RMSEs are plotted against the corresponding (-) root-CRLBs.

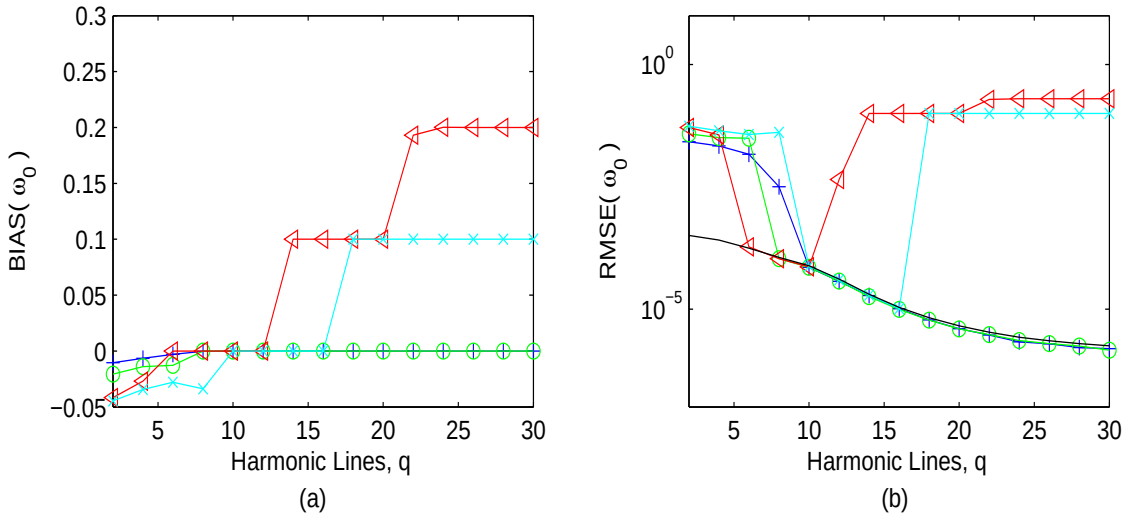

Figure 6: FFE results for the $1/\sqrt{\omega}$ amplitude model versus the true number of harmonics in correlated noise: FFE (a) bias and (b) RMSE. The estimates are generated using the (+) NLS-MDL, ($\circ$) ANLS-MDL, ($\triangleleft$) NLS with r = 10, and ($\times$) NLS with r = 16. The RMSEs are plotted against the (-) root-CRLB for FFEs.

The RMSEs for the higher harmonics ($i.e.$, $\hat{\alpha}_k$ and $\hat{\phi}_k$, for $k = \{5, 10\}$), given in [16], are shown to behavior similar to the RMSEs in Figures 5(c) and (d). Also, although the FFE bias evident in Figure 5(a) is insignificant compared to the true value, it is shown in [16] that the bias decreases with increasing data length.

5.1.2 Algorithm Performance versus the Number of Harmonics in Colored Noise

Now, the performance is compared to the CRLBs as a function of the true number of harmonics in colored noise. The number of harmonics considered is $q \in [2, 30]$ in increments of 2. The orders of the NLS method are fixed at $r = 10$ and 16. The data length is set to $N = 256$. The noise variance is adjusted as described in Section 5.1.1 for a desired SNR of $\rho = 10$ dB.

The bias and RMSE of the FFEs are plotted in Figures 6(a) and (b), respectively. From Figure 6(b), it is observed that RMSEs of the NLS-MDL and ANLS-MDL methods correspond well with the CRLB when $q \geq 8$. However, only 16.8% of the FFEs from ANLS-MDL and 3.4% from NLS-MDL are close to $\omega_0/4$ when $q = 6$. Again, the outlying FFEs, which attribute to the increased RMSE, correspond to outlying order estimates. These percentages are improved compared to the white noise case and worse than those in the uniform amplitude case [16].

The NLS methods with fixed orders only perform well over a small range of q. The estimate variances coincide with the CRLBs only in the ranges $6 \leq q \leq 10$ for NLS with $r = 10$ and $10 \leq q \leq 16$ for NLS with $r = 16$. Outside these ranges, the estimates become biased toward sub- and super-harmonics. This suggests that the performance of the NLS method is comparable to the CRLB as long as the fixed order is in the range $q \leq r < 2q$.

5.2 Field Measurement Data

The following example is a comparison between the STFT and parameter and order estimates using ANLS-MDL from measured data. The field data consists of noise due to the local environment and a single source generating coupled harmonics and un-modeled broadband energy. The source is a heavy-tracked battlefield vehicle. The data was collected at APG, as part of the U.S. Army Research Laboratory's ATR acoustic database, using a seven-sensor, circular microphone array.

The data was recorded at $T = 1/1024$ seconds/sample. The noise is assumed to be stationary and is modeled as a fifth-order ($p = 5$) AR process. The AR parameters are generated using the first 10 seconds ($M = 10\ 240$ samples) of data using the least-squares method given in [10]. The data length for the STFT is $N = 1024$, whereas the data length for ANLS-MDL is $N = 512$. Non-overlapping rectangular windows are used for both the STFT and ANLS-MDL. The frequency and order search regions are the same as those itemized in Section 5.1. In contrast, the minimum allowable order is set to $r_{min} = 0$. The frequency loss function is averaged using data from all seven sensors, as briefly discussed in Section 3.4. Consequently, amplitude and phase estimates are generated from each sensor's data. However, only the results from Sensor 1 are presented.

The STFT of the raw data from Sensor 1 is represented by a spectrogram in Figure 7(a). In Figure 7(b), the harmonic frequency estimates from each half-second data block are plotted along the vertical axis. The horizontal axis represents the progression of time. The relative amplitudes of the spectral data are scaled in decibels.

Up to approximately 200 seconds, ANLS-MDL estimates, for the most part, that there is no harmonic signal. Beyond 200 seconds, it appears the ANLS-MDL frequency and amplitude estimates are well-related to the measured harmonic source. The range of the source from the sensor array at 200 seconds is approximately 1 km. The closest point of approach (CPA) of the source occurs at 380 seconds. The estimates from ANLS-MDL also appear to improve up to and beyond the CPA.

The parameters are generated using independent half-second blocks of data. Although the parameter estimates are independent from block to block, there is an obvious continuity in the low to mid-range harmonics over time, as seen in Figure 7(b).

Using a CLEAN type approach, the signal estimates are subtracted from the whitened data, resulting in the residual signal. The spectrogram for the residual data is shown in Figure 8. As seen in the figure, most of the remaining energy corresponds to un-modeled broadband energy and a pair of possibly coupled harmonic lines.

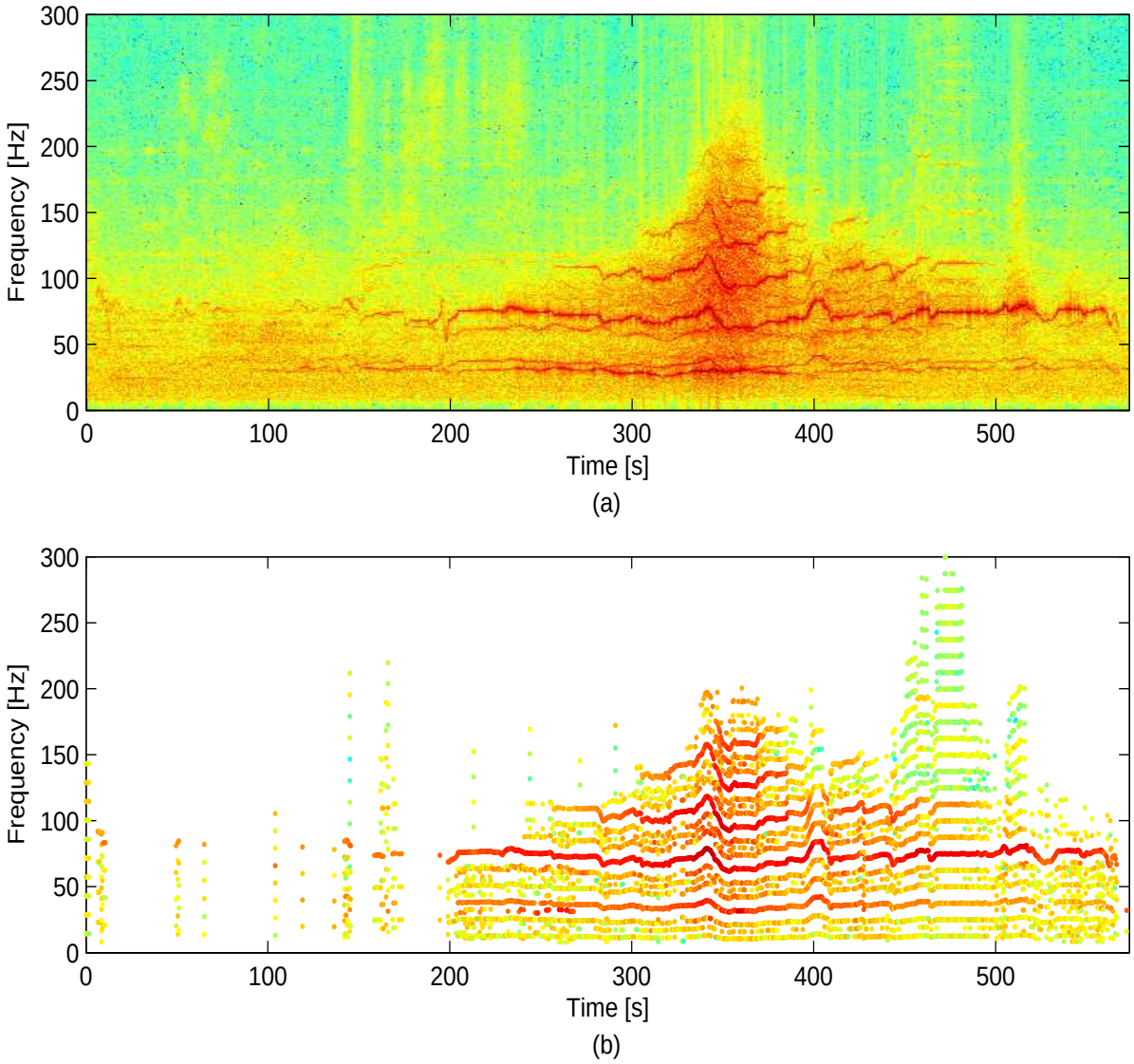

Figure 7: Spectrogram (a) and harmonic line estimates (b) of the acoustic signature from a single heavy-tracked vehicle.

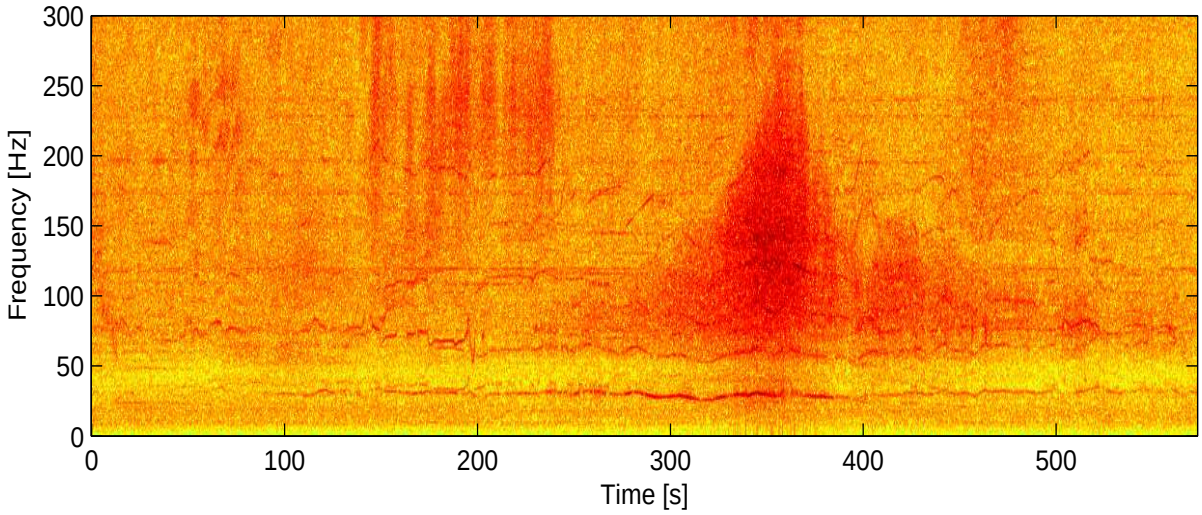

Figure 8: Spectrogram of the residual whitened signal.

6. Conclusions

Two algorithms have been introduced which combine parameter estimation and order selection for coupled harmonic signals in Gaussian noise. These methods and the standard NLS method with a fixed order were evaluated in numeric simulations. The NLS method with $r = q$ corresponds to the maximum likelihood estimator. However, NLS with order selection ($i.e.$, NLS-MDL) exhibits only slight loss in performance compared to the MLEs, and at the expense of computational complexity. The loss in performance is accredited to the uncertainty in the true number of harmonics. However, the performance differences quickly diminish with increasing SNR and data length. Additionally, the ANLS-MDL method offers similar performance to NLS-MDL with fewer computations.

Each algorithm has an associated SNR and sample length thresholds (data length thresholds are shown in [16] to be $N > 256$ for $\rho = 0$ dB). For sufficient SNR and data length, the NLS method provides statistically efficient estimates when the number of harmonics is known. However, when the number of harmonics is not known, but the system order is fixed, the NLS method still provides statistically efficient estimates provided $q \leq r < 2q$. Also, when the number of harmonics is not known, the proposed algorithms provide statistically efficient estimates for sufficient SNR, data length, and harmonic lines. In battlefield acoustics, the number of harmonics is generally not known and the number can vary, as seen in Figures 1 and 7.

In conclusion, the proposed algorithms are efficient methods that can be used to extract features, such as the FF or phase parameters, of single sources generating coupled harmonics. These features are useful in target classification [1] or in DOA estimation. In addition, these algorithms can also be used to initialize and periodically update algorithms designed to track time-varying parameters, which generally require prior knowledge of the number of parameters to track. In the case of multiple sources, these algorithms can be combined with beamforming to temporally and spatially separate targets.

Acknowledgement

Any opinions, findings, and conclusions or recommendations expressed in this publication are those of the authors and do not necessarily reflect the views of the U.S. Army Research Laboratory or the U.S. Government.

References

[1] M. Wellman, N. Srour, and D. Hillis, "Acoustic Feature Extraction for a Neural Network Classifier," *ARL Tech. Report*, vol. ARL-TR-1166, pp. 11–12, Jan 1997.

[2] D. Lake, "Efficient Maximum Likelihood Estimation of Multiple and Coupled Harmonics," *ARL Tech. Report*, vol. ARL-TR-2014, Dec 2000.

[3] A. Nehorai and B. Porat, "Adaptive Comb Filtering for Harmonic Signal Enhancement," *IEEE Trans. Acous., Spch., and Sig. Proc.*, vol. 34, pp. 378–392, Oct 1986.

[4] B. James, B. D. O. Anderson, and R. Williamson, "Conditional Mean and Maximum Likelihood Approaches to Multiharmonic Frequency Estimation," *IEEE Trans. Sig. Proc.*, vol. 42, pp. 1366–1375, Jun 1994.

[5] A. Ferrari, G. Alengrin, and C. Theys, "Estimation of the Fundamental Frequency of a Noisy Sum of Cisoids with Harmonic Related Frequencies," in *IEEE Int. Conf. Acous., Spch., and Sig. Proc.*, vol. 5, pp. 515–520, 1992.

[6] F. Dommermuth, "Estimation of Fundamental Frequencies," *IEE Radar and Sig. Proc.*, vol. 140, pp. 162–170, Jun 1993.

[7] S. Kay and V. Nagesha, "Extraction of Periodic Signals in Colored Noise," in *IEEE Int. Conf. Acous., Spch., and Sig. Proc.*, vol. 5, pp. 281–284, 1992.

[8] J. Rissanen, "Modelling by the Shortest Data Description," *Automatica*, vol. 14, pp. 465–471, 1978.

[9] T. Pham and B. Sadler, "Wideband Acoustic Array Processing to Detect and Track Ground Vehicles," in 130^{th} *meeting of the Acoustical Society of America*, Nov 1995.

[10] P. Stoica and R. Moses, *Introduction to Spectral Analysis*. Upper Saddle River, NJ: Prentice Hall, 1997.

[11] P. Stoica, A. Jakobsson, and J. Li, "Cisoid Parameter Estimation in the Colored Noise Case: Asymptotic Cramér-Rao Bound, Maximum Likelihood, and Nonlinear Least-Squares," *IEEE Trans. Sig. Proc.*, vol. 45, Aug 1997.

[12] P. Stoica and A. Nehorai, "Statistical Analysis of Two Non-Linear Least-Squares Estimators of Sine Waves Parameters in the Colored Noise Case," in *IEEE Int. Conf. Acous., Spch., and Sig. Proc.*, vol. 4, pp. 2408–2411, 1988.

[13] P. Stoica, R. Moses, B. Friedlander, and T. Söderstrom, "Maximum Likelihood Estimation of the Parameters of Multiple Sinusoids from Noisy Measurements," *IEEE Trans. Acous., Spch., and Sig. Proc.*, vol. 37, pp. 378–392, Mar 1989.

[14] A. Swami and M. Ghogho, "Cramér-Rao Bounds for Coupled Harmonics in Noise," vol. 1, pp. 483–487, Nov 1997.

[15] M. Ghogho and A. Swami, “Lower Bounds on the Estimation of Harmonics in Colored Noise,” vol. 1, pp. 478–482, Nov 1997.

[16] G. Whipps, “Coupled harmonics: Estimation and detection,” Master’s thesis, The Ohio State University, 2003.

[17] P. Djurić, “A Model Selection Rule for Sinusoids in White Gaussian Noise,” *IEEE Trans. Sig. Proc.*, vol. 44, pp. 1744–1751, Jul 1996.

[18] A. Sabharwal, C. Ying, L. Potter, and R. Moses, “Model Order Selection for Summation Models,” 13^{th} *Asilomar Conf. Sig., Sys., and Comp.*, vol. 2, pp. 1240–1244, Nov 1996.

[19] X. Wang, “An AIC Type Estimator for the Number of Cosinusoids,” *Journal of Time Series Analysis*, vol. 14, no. 4, pp. 433–440, 1993.

[20] M. Wax and T. Kailath, “Detection of Signals by Information Theoretic Criteria,” *IEEE Trans. Sig. Proc.*, vol. 33, pp. 387–392, Apr 1985.